

# STRAIN MONITORING ON A COMPOSITE AIRCRAFT CABIN WITH FIBER OPTIC SENSORS

Patricia F. DÍAZ-MAROTO<sup>1\*</sup>, Antonio FERNÁNDEZ<sup>1</sup>, Rosario FERNÁNDEZ<sup>2</sup>,  
Nicolás GUTIÉRREZ<sup>2</sup>, Fernando LASAGNI<sup>2</sup>, J. Alfredo GÜEMES<sup>1</sup>

<sup>1</sup>Laboratory of Composite Materials and Smart Structures, Dpt. Aeronautics, UPM  
Plaza Cardenal Cisneros, 3 - Madrid 28040 SPAIN. [p.fernandezdm@aero.upm.es](mailto:p.fernandezdm@aero.upm.es)

<sup>2</sup> Materials & Processes department, Center for Advanced Aerospace Technologies (CATEC)  
C/Wilbur y Orville Wright 17-19-21, E-41309 La Rinconada, Seville, SPAIN.

**Key words:** Fiber Optic, FBG, Distributed sensing, Aerospace SHM applications.

## Abstract

An integral composite aircraft cabin had been instrumented with two different technologies: distributed fiber optic sensors (DFOs) and Fiber Bragg Gratings (FBGs). This structural test aims at strain field monitoring in any part of structure when cabin pressurization is applied in order to simulate flight conditions.

The Distributed fiber optic network used is based on Rayleigh scattering using an Optical Backscatter Reflectometer (OBR). The OBR provides a large number of strain sensors with high spatial and strain accuracy with a plain optical fiber. DFOs prove to be the most suitable technology for this test due to their capability to cover large areas with an important amount of strain data.

Moreover, the technology of Fiber Bragg Grating sensors has been also applied for the monitoring of the cabin structural integrity. This type of sensors enable a continuous monitoring during the pressurization tests. 24 FBG sensors in four fiber optic circuits were installed on cabin surface.

This test allows to correlate distributed and discrete fiber optic sensors and evaluate their damage detection capabilities. Several static pressure tests were conducted in order to detect structural damage and static loads at the cabin structure.

## 1 INTRODUCTION

Composite materials have a high structural integration capability that allows to manufacture complex structures without rivets or additional joining elements. In the aeronautic industry this advantage is one of the most important requirements since it represents important weight and manufacturing costs savings. For that reason, an integral composite aircraft cabin have been developed not only to compare with traditional methods of manufacturing but also to verify the structural integrity with one of the most powerful technology that exists for testing nowadays, fiber optic sensors [1-3]. Optical sensors have been proved as an alternative in structural test as they provide a more specific approach of strain field than conventional sensors such as electrical strain gauges.



This project is focused on a structural test monitoring by means of an optical sensor network based on FBGs and distributed sensing using Rayleigh scattering.

## 2 DISTRIBUTED FIBER OPTIC SENSING

The distributed sensing network was carried out using an Optical Backscatter Reflectometer (OBR) equipment to measure the Rayleigh scattering. The OBR is an optical frequency domain reflectometer (OFDR) that uses a swept-wavelength interferometry by means of a tunable laser to interrogate the device under test (DUT) with very high spatial resolution [4, 5]. This powerful technique allows to obtain a strain measurement each 5 mm with a high resolution of  $10\mu\epsilon$ . An OBR schematic is shown in Figure 1.

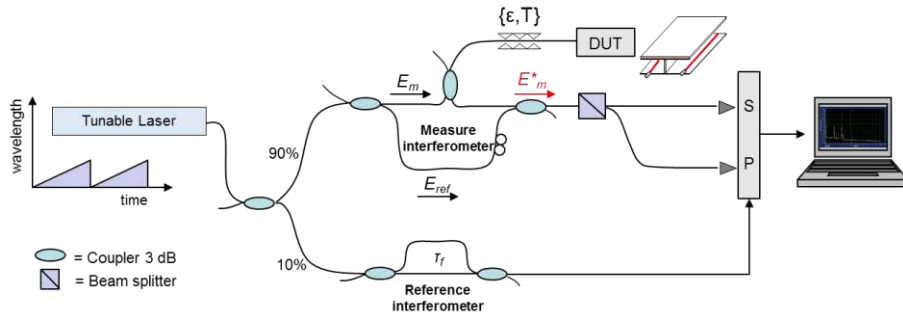


Figure 1: Schematic of Optical Backscatter Reflectometer.

Rayleigh scattering is caused by random fluctuations in the refractive index when fiber optic is manufactured. The OBR is an optical frequency domain reflectometer (OFDR) that uses a swept-wavelength interferometry to obtain the total reflected spectrum with high spatial resolution. When a segment of fiber optic is strained or heated then reflected spectrum experiences a shift. A cross-correlation is performed in order to determine the spectral shift between two different DUT conditions. One of them considered as a reference state and other recorded as a strained state. The amount of spectral shift is linearly dependent on temperature and strain changes, see Figure 2.

$$\frac{\Delta\lambda}{\lambda_0} = -\frac{\Delta\nu}{\nu_0} = K_T\Delta T + K_\epsilon\Delta\epsilon \quad (1)$$

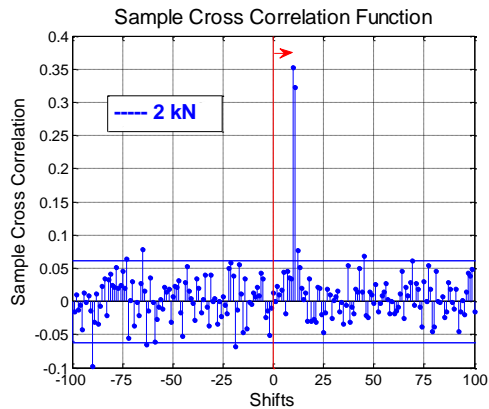


Figure 2: Frequency shift calculated for a strained sensor under 2kN tensile force by means of a cross correlation function. The equation is the relationship between strain or temperature changes and the amount of spectral shifts.

All shifts are calculated in a sensing range by lots of cross-correlation for each gauge length segment along the DUT, with the purpose to obtain a distributed strain measurement.

### 3 FIBER BRAGG -GRATING

A Fiber Bragg Grating sensor is a short segment of fiber optic in whose core multiple transverse stripes have been engraved periodically. These stripes cause that the core refraction index changes along the longitudinal direction [6, 7]. The FBG sensor performance is similar to an optical filter: one specific wavelength is reflected and the rest of the incident spectrum is transmitted. This wavelength is defined by the equation (2):

$$\lambda_B = 2\Lambda n_0 \quad (2)$$

Where  $\lambda_B$  is the wavelength,  $\Lambda$  is the modulation period and  $n_0$  is the mean refraction index. If the sensor is exposed to mechanical or thermal deformation, the characteristic wavelength changes proportionally to the applied deformation. Measuring the variation experimented by the reflected wavelength enables to calculate the deformation [8-11]. The optical sensing interrogator Micron Optics SM130-700 has been used for the monitoring and measuring of strain state with FBG sensors. It is built upon the X30 optical interrogator core, featuring a high power and high speed swept wavelength laser, which allows a large data acquisition coming from multiple sensors.

### 4 EXPERIMENTAL SET-UP

Both technologies of fiber optics sensors, OBR and FBGs, were installed to monitor the full scale pressurization test on a composite aircraft. The evolution of the strain status has been registered by means of this dense network spread out on the element surface. Optical sensors were placed in the most interesting regions, where maximum stress values are reached, e.g. high stress areas due to the influence of doors or windows corners as well as riveted zones. Furthermore, these points are coincident with strain gauge locations, which provide a reference value for optical network measurements.

#### 4.1 Distributed sensing network

Distributed sensing network were performed in 5 paths. Four of them covered all cabin surface both sides. Moreover, this configuration was chosen since the most critical areas were close to these paths. A schematic representation is shown in Figure 3.

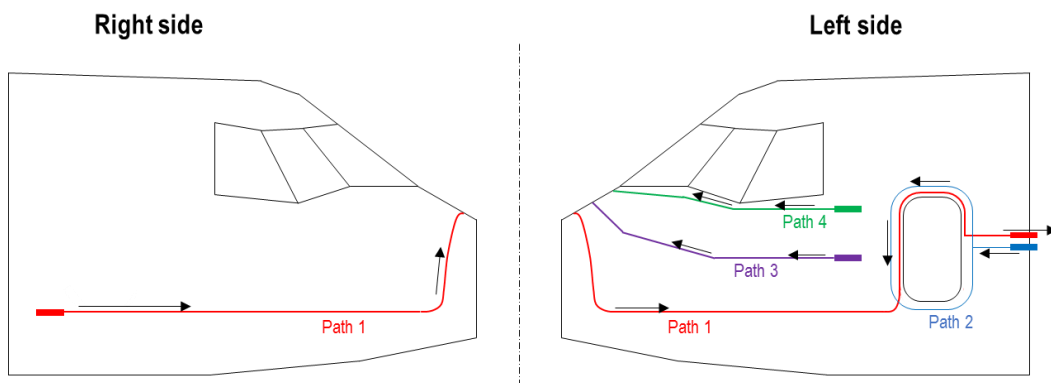


Figure 3: Distributed fiber optic sensors placed on cabin surface organized in 4 paths.

Another path was placed in the torsion box. This structure was manufactured in aluminum alloy and the behavior obtained under the pressurization load have been different. Fiber optic path cover both box faces by means of several sensing lines.

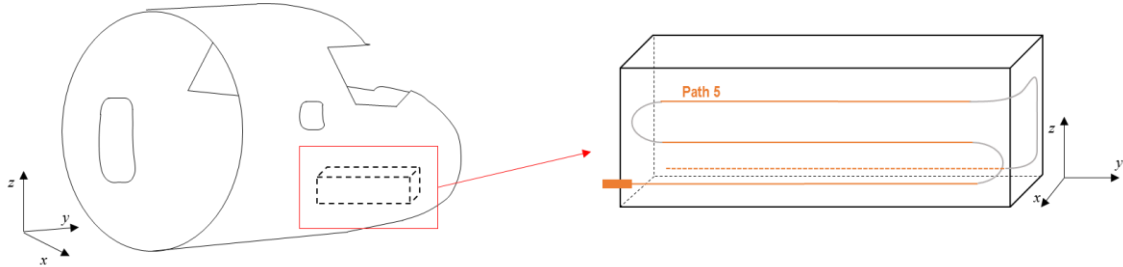


Figure 4: Path 5 of distributed sensors placed in the torsion box.

## 4.2 Fiber Bragg Grating Network

The FBG network have four measurement channels, as this the maximum number of fiber optics that can be connected at the same time. Based on this, the final FBG distribution on cockpit surface is shown in Figure 5, where sensor positions are indicated with blue dots over the lines which represent the fiber optic paths. Strain gauges locations are represented as well.

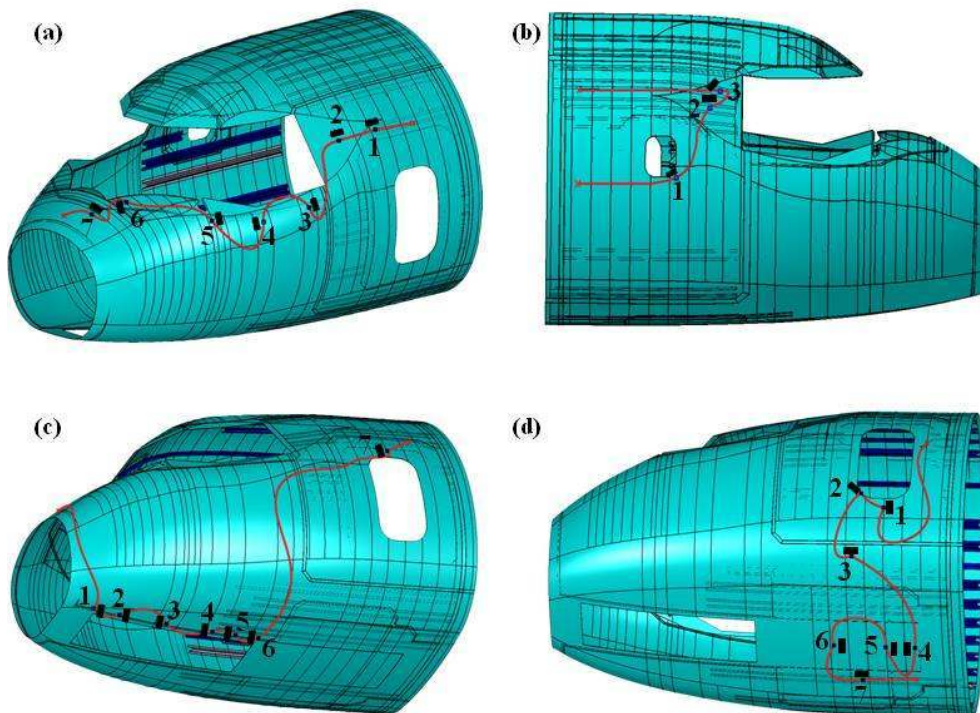


Figure 5: Fiber optic circuits: (a) line 1, (b) line 2, (c) line 3 and (d) line 4. Strain gauges positions are represented by rectangles.

Fiber optic lines were manufactured ad-hoc for this application. As can be observed in Figure 5, fiber distribution spans the entire cockpit surface except the ceiling area, due to the lack of access to this region.

## 5 RESULTS

A pressurization test was carried out over the cockpit in order to evaluate its structural integrity. The maximum inner pressure applied was 3 psi. This value was reached through eight pressure steps: 1, 1.5, 1.75, 2, 2.25, 2.5, 2.75 and 3 psi. The structural integrity of the component was checked and verified in each load increment. After that, pressure was released up to 0.29 psi, by means of the valves opening. A second pressurization test was performed, reaching a maximum value of 1.5 psi with the subsequent complete depressurization.

### 5.1 Distributed sensing Network

Measurements were acquired through Optical Backscatter Reflectometer equipment. OBR's software saves data in a binary format which records lots of information. For distributed fiber optic technology the structural test was stopped at each loading step since measurement acquisition needs few seconds to carry out.

Figure 6 shows the strain level all along the first fiber optic path. The highest level was measured around the door, where the strains are significantly higher than on surface skin. Furthermore, reinforcement's zones are noticeable in the sensor signal since strain level is decreased.

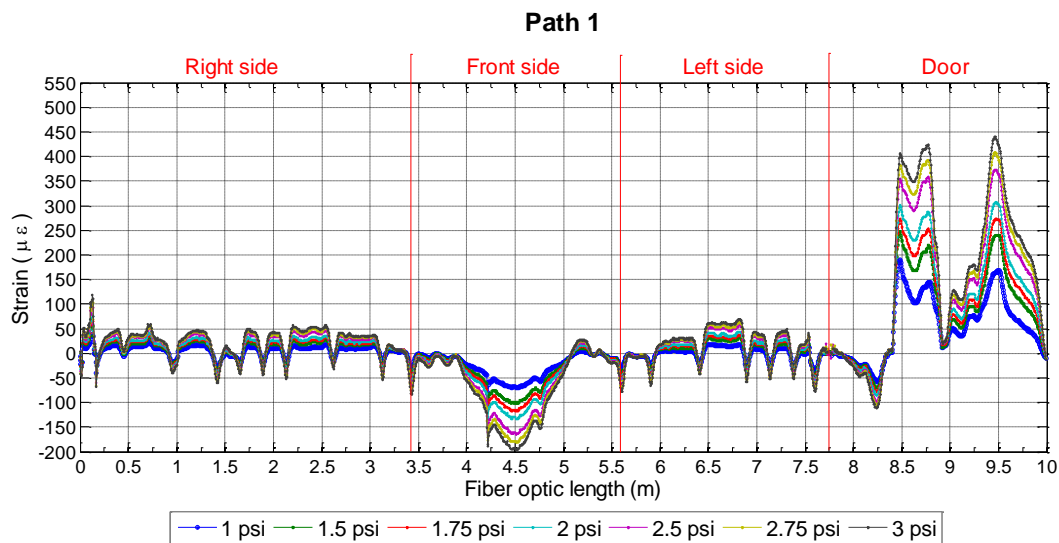


Figure 6: Strain profile all along of fiber optic path 1.

The most remarkable behaviour during the pressurization test was registered in the torsion box. Thanks to distributed strain measurement a local buckling has been detected during pressurization test. In contrast to punctual sensors which cannot provide the full information of the strain field, DFOS allows to detect buckling and high loading areas. In order to carry out a visual buckling representation on 2D view a signal post-processing has been performed as a strain map of the measured information.

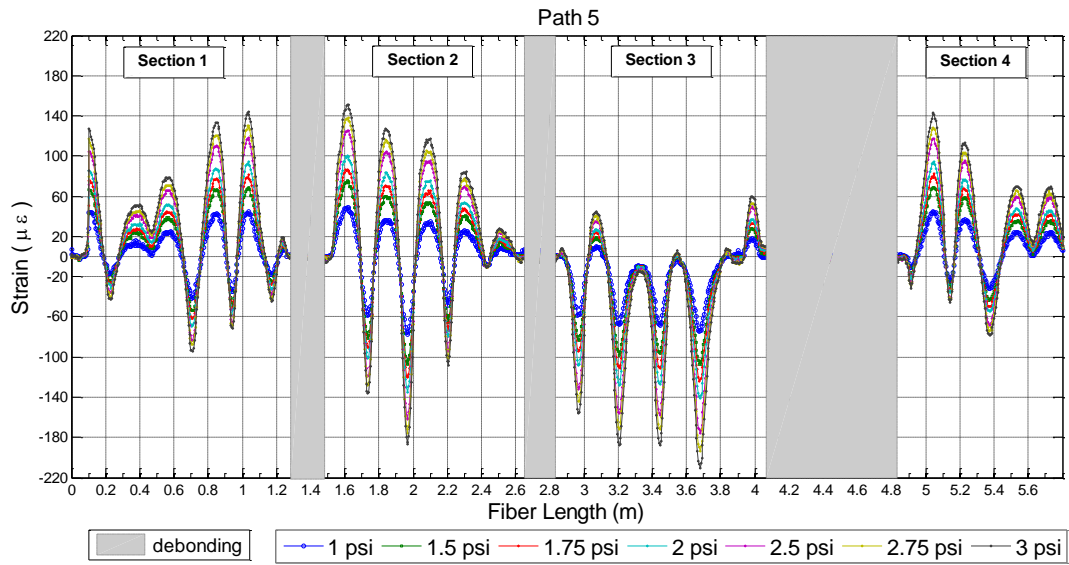


Figure 7: Strain field of fiber path 5 along torsion box face.

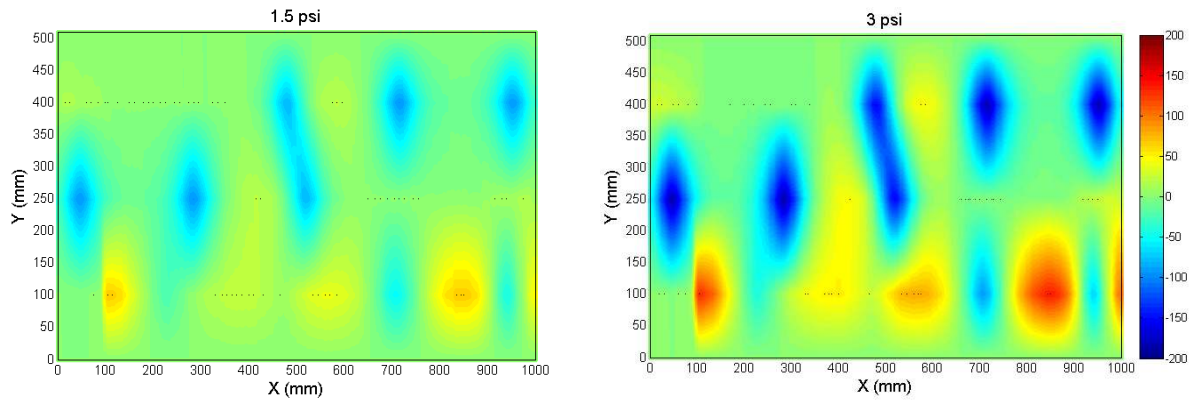


Figure 8: Strain color-map representation for buckling detection inside the torsion box.

## 5.2 Fiber Bragg Grating Network

FBG sensor measurements are represented in Figure 9, where each graphic corresponds to one fiber circuit. The inner pressure value has been overlapped, allowing relating the load state with the strain distribution.

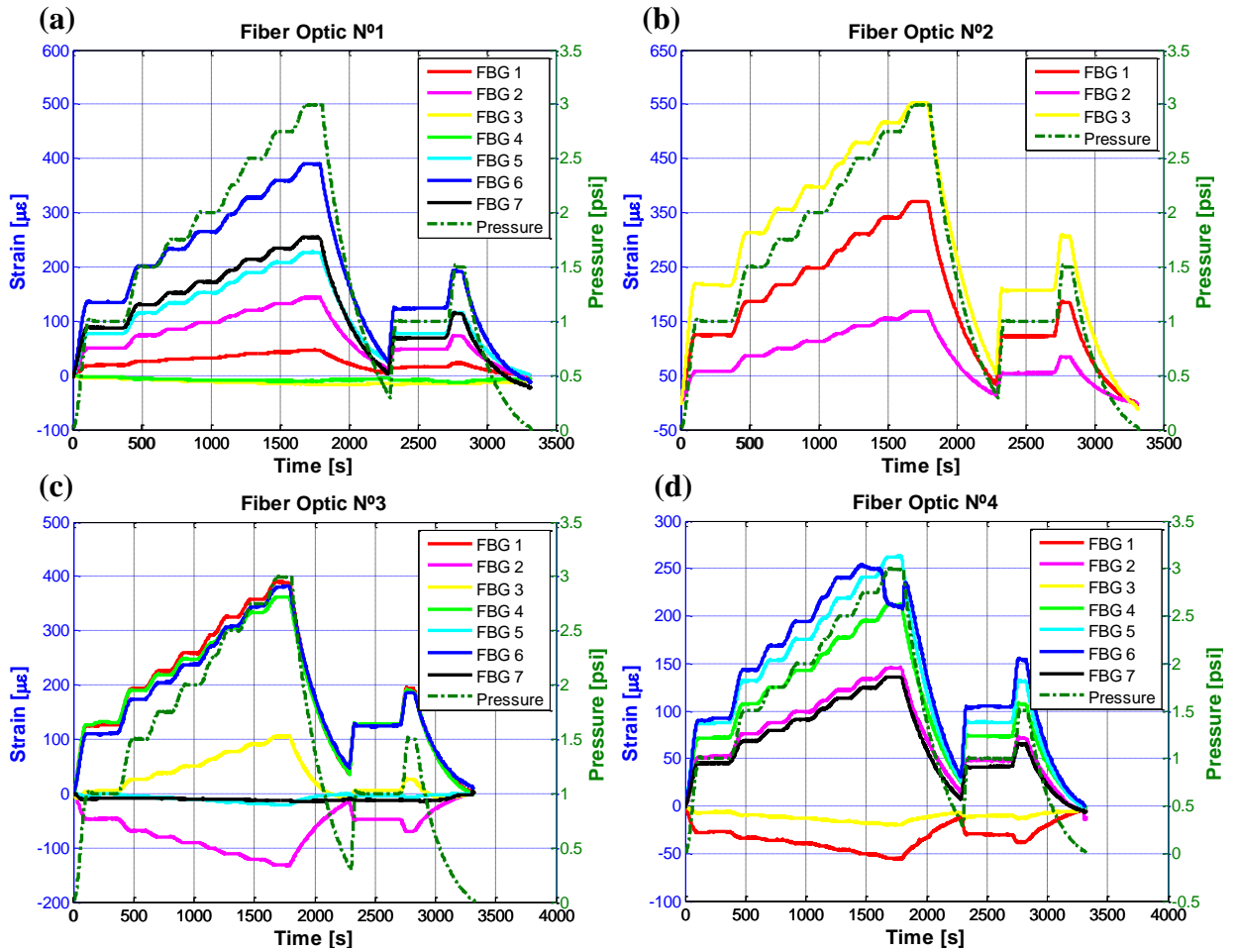


Figure 9: FBG sensor measurements during pressurization tests up to 3 psi.

The analysis of FBG sensor records enables to identify the load increments. Maximum positive strain values was detected in FBG N°3 of fiber optic N°2 (553  $\mu\epsilon$ ), corresponding to the sensor located closest to the cockpit ceiling. The minimum value was registered by sensor N°2 of fiber optic circuit N°3 (-132  $\mu\epsilon$ ). This sensor was situated near to the landing gear hole. Both values were measured when the inner pressure was 3 psi.

Table 1 shows the comparison between FBG measurements and strain gauges records, for an applied pressure of 3 psi.

Circuit	Sensor type	N° 1	N° 2	N° 3	N° 4	N° 5	N° 6	N° 7
		[ $\mu\epsilon$ ]	[ $\mu\epsilon$ ]	[ $\mu\epsilon$ ]	[ $\mu\epsilon$ ]	[ $\mu\epsilon$ ]	[ $\mu\epsilon$ ]	[ $\mu\epsilon$ ]
1	FBG	47	143	-17	-10	227	389	253
	SG	23	168	-124	-159	-26	397	171
2	FBG	370	167	553	-	-	-	-
	SG	707	195	401	-	-	-	-
3	FBG	389	-132	105	361	-21	381	-13
	SG	378	-90	-207	-215	-35	349	13
4	FBG	-56	145	-20	212	262	210	136
	SG	-36	376	-29	150	120	188	169

Table 1: Strain measurements with FBG and strain gauge sensors at 3 psi.

Significant differences between both values are detected in some cases, even registering strain values with opposite sign. In most of them, these discrepancies are promoted by the distance between both types of sensors. For example, for FBG N°4 of fiber optic circuit N°3, this distance exceeds 15 cm.

In fiber lines N°2 and N°3, the maximum differences are registered by the couple of sensors identified by numbers 1 and 2, respectively. In both cases, the measuring devices are located in a region under the effect of a stress concentrator (window and door corners). Although FBG sensors were positioned as proximate as possible to strain gauges, the presence of stress concentrators can cause large strain changes in short distance, as can be distinguished in Table 1.

Finally, great differences are observed in sensors N° 5 (fiber optic circuit N°1). In this case, strain gauge was fixed in a riveted region, where a frame is joined with the cockpit skin. In spite of distance between both devices was lower than 2 cm, the fiber sensor was attached out of the riveted area, having as a consequence large differences between the strain records.

## 6 CONCLUSIONS

A total of 5 distributed sensing lines and 24 FBG sensors were installed on the composite cabin surface obtaining a dense optical sensing network around the structure. The strain field was successfully registered with the fiber optic sensors during pressurization test, being possible to identify the applied load steps and high local strain concentrations. Moreover, it was verified that structural damage was not detected after the test since sensors signal showed a normal behaviour without residual strain. Optical sensor network has been proved to be as an alternative to conventional strain sensors such as strain gauges. In comparison with them, fiber optic sensors afford a significant reduction in terms of integration and installation time, in addition to eliminate the electric wires required for the operation and it also offers significant weight savings.

In conclusion, fiber optic sensors is a powerful technology for structural tests that may be monitored with major improvements in terms of spatial and strain resolution, detection of high local strained areas and the ease of network installation.

## REFERENCES

- [1] Criado, A., Riezu, M., Fernandez, A. and Oizm, A. 2009. "Evaluation of OBR for strain measurements in blade testing". Proceedings of European Wind Energy Conference, Marseille, France.
- [2] Güemes, J A., Menendez, J M., Frovel, M., Fernandez, I., Pintado, J M. 2001 "Experimental analysis of buckling in aircraft skin panels by fibre optic sensors" Smart Materials and Structures Vol. 10, no. 3, pp. 490-496.
- [3] F. Diaz-Maroto, P., Fernandez-Lopez, A., Güemes, J A., "Distributed fibre optic sensors for stiffened skin panels strain monitoring and failure mode detection" Proceedings of the 10th International Workshop on Structural Health Monitoring 2015, Stanford, California



- [4] Soller, B J., Wolfe, M., and Froggatt, M. E. 2005 “Polarization resolved measurement of Rayleigh backscatter in fiber-optic components.” Optical Fiber Communication Conference and Exposition and the National Fiber Optic Engineers Conference Technical Digest. Anaheim, California.
- [5] Güemes, J A, Fernandez-Lopez, A., Soller B. 2010 “Optical Fiber Distributed Sensing. Physical Principles and Applications” J. Structural Health Monitoring, Vol. 9, No. 3, 233-245.
- [6] Luyckx, G., Voet, E., Lammens, N., Degrieck, J., Strain Measurements of Composite Laminates with Embedded Fibre Bragg Gratings: Criticism and Opportunities for Research. Sensors, **11**, 384-408,2011.
- [7] Hill, K.O., Meltz, G., Fiber Bragg Grating Technology Fundamentals and Overview. Journal Lightwave Technology, **15**, 1263–1276, 1997.
- [8] Mawatari, T., Nelson, D., A Multi-Parameter Bragg Grating Fiber Optic Sensor and Triaxial Strain Measurement. Smart Materials and Structures, **17**, 035033, 2008.
- [9] Tanaka, N., Okabe. Y., Takeda, N., Temperature-Compensated Strain Measurement using Fiber Bragg Grating Sensors Embedded in Composite Laminates. Smart Materials and Structures, **12**, 940-946, 2003.
- [10] Guemes, J A., Menendez, J M., Response of Bragg Grating Fiber-Optic Sensors when Embedded in Composite Laminates. Composite Science Technology, **62**, 959-966, 2002.
- [11] Surrea, F., Scott, R H., Banerji, P., Basheer, P.A.M., T. Sun, T., Grattan, K. T.V., Study of Reliability of Fibre Bragg Grating Fibre Optic Strain Sensors for Field-Test Applications. Sensors and Actuators A, **185**, 8-16, 2012.